

Performance of Regenerative Relay-Assisted D2D Communication in Mixed Fading Channels

Dharmendra Dixit^{ID} and P. R. Sahu, *Member, IEEE*

Abstract—Performance of device-to-device communication using selective decode-and-forward relaying is analyzed in mixed two-wave with diffuse power and Nakagami- m fading channels. A relay that successfully decodes the source information forwards it to the destination. The destination device combines the direct message signal from the source and its copy via the relay using maximal-ratio combining. Novel closed-form expressions for exact and asymptotic average bit error rates are derived. Furthermore, diversity order, the coding gain, and the optimal power allocation factor are obtained for better system insights. The analysis has been verified through Monte Carlo simulations.

Index Terms—Regenerative relay, device-to-device, decode-and-forward, average bit error rate, mixed fading.

I. INTRODUCTION

FUTURE of mobile communication is tending towards device-to-device (D2D) centric [1]. D2D communication assisted by cooperative relaying has received attention as it can enhance spectral efficiency and energy efficiency needed for fifth generation (5G) mobile standards [2]. In the regenerative selective decode-and-forward (DF) protocol based cooperative communication, the relay device decodes a received signal from the source device and then encodes and transmits it to the destination device [3].

Two-wave with diffuse power (TWDP) fading and Nakagami- m fading are two generalized fading distributions that model practical fading channels with high accuracy. The TWDP fading model consists of two line-of-sight (LoS) multipath components in the presence of diffusely propagating waves [4]. Analyzing the empirical data from static wireless sensors, TWDP fading model has been verified to fit to practical frequency-selective fading and “indoor and outdoor” LoS environments. The well known Nakagami- m fading model fits best to land-mobile and indoor-mobile multipath propagation [5].

A more accurate practical fading scenario model, termed as *mixed fading*, can accommodate wide range of wireless propagation scenarios, suitable to model practical urban micro-cell and indoor wireless scenarios [6]. It can be viewed as generalization of the independent non-identically distributed (i.n.d) symmetric fading channels. Practical D2D links in urban areas (especially in malls, restaurants, public gatherings etc.) can be under mixed fading, i.e., one or more links are dominated by strong LoS components relative to other

Manuscript received November 7, 2017; revised December 28, 2017; accepted January 14, 2018. Date of publication January 26, 2018; date of current version April 7, 2018. The associate editor coordinating the review of this paper and approving it for publication was P. Patras. (*Corresponding author: Dharmendra Dixit.*)

The authors are with the School of Electrical Sciences, IIT Bhubaneswar, Bhubaneswar 752050, India (e-mail: dd12@iitbbs.ac.in; prs@iitbbs.ac.in).

Digital Object Identifier 10.1109/LCOMM.2018.2798670

links [6]. Hence, performance analysis of D2D cooperative communications under mixed fading, has received research attention [6]. Several works on the performance analysis for D2D communication assisted by DF relaying over different fading channels are available in literature; the ones in line with the perspective of this work are [7]–[14]. The rich applicability and generality of practical mixed TWDP and Nakagami- m fading environments for D2D communication, deserves its performance analysis for DF relaying cooperative communication scheme, which as per authors’ literature survey would contribute to reasonably fill the research gap in the current literature.

In this letter, average bit error rate (ABER) performance of selective DF relay assisted D2D communication over mixed TWDP and Nakagami- m fading channels is investigated. Following are the main contributions of the work presented herewith: a) novel closed-form expressions for both exact and asymptotic ABER for coherent modulation schemes, b) expressions for the diversity order, coding gain, and optimal power allocation factor. It can be noted that the derived ABER expressions accommodate mixed Nakagami- m and Rician, mixed hyper-Rayleigh and Nakagami- m , and symmetric Rayleigh fading channel scenarios as special cases.

The rest of the letter is organized as follows. Section II includes system and channel model. The performance analysis is presented in Section III. In Section IV, numerical results and discussion are presented. The letter is concluded in Section V.

II. SYSTEM AND CHANNEL MODEL

We consider classical three-device model which is an appropriate model for relay assisted D2D communication [1], where a source device ‘ s ’ sends its message in two consecutive time slots, to a destination device ‘ d ’ using a single relay device ‘ r ’. In selective DF relaying, if the decoded message at ‘ r ’ is correct, the message is sent to ‘ d ’ in the second time slot. Correct decoding at ‘ r ’ can be achieved by using cyclic-redundancy-check codes or threshold-based checking [9]. Here, the device ‘ k ’ sends its information to the device ‘ l ’ over kl link, where $k \in \{s, r\}$, $l \in \{r, d\}$ and $kl \in \{sd, sr, rd\}$. When unit energy symbol x is transmitted from ‘ k ’, the received signal at ‘ l ’ can be given as $y_{kl} = \sqrt{\bar{P}_k} \alpha_{kl} x + n_{kl}$, where \bar{P}_k is the transmission power per symbol at ‘ k ’, α_{kl} is the fading channel coefficient of kl link which is modeled as either TWDP or Nakagami- m distribution, and n_{kl} is additive white Gaussian noise with N_0 variance at ‘ l ’. The instantaneous signal-to-noise ratios (SNR) of the kl link can be given by $\gamma_{kl} = \alpha_{kl}^2 \bar{P}_k / N_0$. At ‘ s ’, the symbol is transmitted with power $\bar{P}_k = P_s$. If ‘ r ’ successfully decodes the received symbol, the symbol is re-transmitted with power $\bar{P}_k = P_r$, otherwise ‘ r ’ remains idle, i.e. $P_r = 0$. $P = P_s + P_r$ is denoting

total end-to-end transmission power per symbol. If decoding is successful at ‘ r ’, the signals at ‘ d ’ are combined using maximal ratio combining and hence, the instantaneous SNR at ‘ d ’ is $\gamma_{mrc} = \gamma_{sd} + \gamma_{rd}$.

The compact moment generating function (MGF) expression of TWDP faded link ‘ kl ’ can be expressed as [10]

$$M_{\gamma_{kl}}(z) = \sum_{j=1}^{2L} \frac{\tilde{b}_{klj} \tilde{K}_{kl}}{2(\tilde{K}_{kl} + z\bar{\gamma}_{kl})} \exp\left(-\frac{z\bar{\gamma}_{kl} C_{klj}}{\tilde{K}_{kl} + z\bar{\gamma}_{kl}}\right), \quad (1)$$

where z is the Laplace transform variable, $\tilde{b}_{kl2i-1} = \tilde{b}_{kl2i} = b_{kl_i}$, $\tilde{K}_{kl} = 1 + K_{kl}$, K_{kl} is the ratio of the total specular power to diffuse (scatter) waves, $C_{kl2i-1} = (1 - \rho_{kl_i})(\tilde{K}_{kl} - 1)$, $C_{kl2i} = (1 + \rho_{kl_i})(\tilde{K}_{kl} - 1)$, $\rho_{kl_i} = \Delta_{kl} \cos((i-1)\pi/(2L-1))$, $i = 1, 2, \dots, L$, Δ_{kl} represents the relative strength of the two specular components, $L \geq \max\{K_{kl}, \Delta_{kl}/2\}$ is the order of the approximate probability density function, $\bar{\gamma}_{kl} = \mathbb{E}[\gamma_{kl}] = \Omega_{kl} \bar{P}_k / N_0$ denotes the average SNR of the kl link, $\mathbb{E}[\cdot]$ is the expectation operator, and $\Omega_{kl} = \mathbb{E}[\alpha_{kl}^2]$ is the mean power of α_{kl} . The values of $\{b_{kl_i}\}_{i=1}^L$ are given in Table II of [4]. The following are special cases of the TWDP: Rayleigh ($K_{kl} = 0$) and Rician ($\Delta_{kl} = 0$).

The MGF expression of Nakagami- m faded link ‘ kl ’ can be given by [5]

$$M_{\gamma_{kl}}(z) = \left(1 + \frac{z\bar{\gamma}_{kl}}{m_{kl}}\right)^{-m_{kl}}, \quad (2)$$

where $m_{kl} \geq 0.5$ is the Nakagami fading parameter. The following are special cases of the Nakagami- m : Rayleigh ($m_{kl} = 1$) and one-sided Gaussian ($m_{kl} = 0.5$).

III. PERFORMANCE ANALYSIS

The conditional BER at ‘ d ’ can be written as [9], [12]

$$\begin{aligned} P(e|\gamma_{mrc}, \gamma_{sr}) &= P(e|\gamma_{sr})P(e|\gamma_{sd}) \\ &\quad + (1 - P(e|\gamma_{sr}))P(e|\gamma_{mrc}). \end{aligned} \quad (3)$$

Assuming the input symbol x to be digitally modulated with coherent detection, the well-known MGF based method can be employed to do BER averaging, i.e. [5]

$$P_v(e) = \mathbb{E}[P(e|\gamma_v)] = \frac{a}{\pi} \int_0^{\frac{\pi}{2}} M_{\gamma_v}\left(\frac{c^2}{2\sin^2\theta}\right) d\theta, \quad (4)$$

where $v \in \{sd, sr, mrc\}$, a and c are two constants determined by the coherent modulation scheme, and $M_{\gamma_v}(\cdot)$ denotes the MGF of γ_v . The ABER expression in (4) is applicable for a number of low to higher order coherent modulation schemes defined by the parameters a and c [5]. Here, the ABER of three-node D2D communication using selective DF relaying is analyzed when the three links are subjected to different fading. One has six combinations of channel links with two fading types. In this work, we consider that sd and sr links are TWDP faded and the rd link is Nakagami- m faded.

A. Exact ABER Analysis

Assuming independent faded links and averaging (3) over the PDF of instantaneous SNRs γ_{sr} , γ_{sd} , and γ_{mrc} , we obtain

$$P(e) = P_{sr}(e)P_{sd}(e) + (1 - P_{sr}(e))P_{mrc}(e), \quad (5)$$

where

$$P_w(e) = \frac{a}{\pi} \int_0^{\frac{\pi}{2}} M_{\gamma_w}\left(\frac{c^2}{2\sin^2\theta}\right) d\theta, \quad w \in \{sr, sd\} \quad (6)$$

$$P_{mrc}(e) = \frac{a}{\pi} \int_0^{\frac{\pi}{2}} M_{\gamma_{sd}}\left(\frac{c^2}{2\sin^2\theta}\right) M_{\gamma_{rd}}\left(\frac{c^2}{2\sin^2\theta}\right) d\theta. \quad (7)$$

The closed-form solutions of $P_w(e)$ and $P_{mrc}(e)$ are given in following subsections. The ABER expressions obtained in the following and subsequent subsections are in terms of the confluent Lauricella’s hypergeometric function, which is defined as [15]

$$\begin{aligned} \Phi_1^{(n)}(m; p_1, p_2, \dots, p_{n-1}; q; z_1, z_2, \dots, z_n) &= \frac{\Gamma(q)}{\Gamma(m)\Gamma(q-m)} \\ &\times \int_0^1 v^{m-1} (1-v)^{q-m-1} \prod_{i=1}^{n-1} (1-vz_i)^{-p_i} \exp(vz_n) dv. \end{aligned} \quad (8)$$

1) *A Closed-Form Solution of $P_w(e)$:* Putting (1) into (6) and using two successive substitutions $u = \frac{2\tilde{K}_w C_{w_j} \sin^2\theta}{2\tilde{K}_w \sin^2\theta + c^2 \bar{\gamma}_w}$ and $v = \left(\frac{2\tilde{K}_w + c^2 \bar{\gamma}_w}{2\tilde{K}_w C_{w_j}}\right) u$, respectively and with the definition of two variable confluent Lauricella’s hypergeometric function $\Phi_1^{(2)}(\cdot)$ for $n = 2$ in (8), we derive the closed form solution of $P_w(e)$ for TWDP faded link given as

$$\begin{aligned} P_w(e) &= 0.25ac\lambda_w^{1.5} \tilde{K}_w \sqrt{\bar{\gamma}_w} \sum_{j=1}^{2L} \tilde{b}_{wj} \exp(-C_{wj}) \\ &\quad \times \Phi_1^{(2)}(1.5; 1; 2; 2\lambda_w \tilde{K}_w, 2\lambda_w \tilde{K}_w C_{wj}), \end{aligned} \quad (9)$$

where $\lambda_w = (2\tilde{K}_w + c^2 \bar{\gamma}_w)^{-1}$.

2) *A Closed-Form Solution of $P_{mrc}(e)$:* Putting (1) and (2) into (7) and using two successive substitutions $u = \frac{2\tilde{K}_{sd} C_{sdj} \sin^2\theta}{2\tilde{K}_{sd} \sin^2\theta + c^2 \bar{\gamma}_{sd}}$ and $v = \left(\frac{2\tilde{K}_{sd} + c^2 \bar{\gamma}_{sd}}{2\tilde{K}_{sd} C_{sdj}}\right) u$, respectively and with the definition of three variable confluent Lauricella’s hypergeometric function $\Phi_1^{(3)}(\cdot)$ for $n = 3$ in (8), we obtain the closed form solution of $P_{mrc}(e)$ for mixed fading scenario such as TWDP faded sd link and Nakagami- m faded rd link given as

$$\begin{aligned} P_{mrc}(e) &= \frac{ac(2\bar{\gamma}_{sd}\lambda_{sd})^{m+1.5} \tilde{K}_{sd} \Gamma(m_{rd} + 1.5)}{\bar{\gamma}_{sd} (\bar{\gamma}_{rd}/m_{rd})^{m_{rd}} \Gamma(m_{rd} + 2)} \sum_{j=1}^{2L} \tilde{b}_{sdj} \exp(-C_{sdj}) \\ &\quad \times \Phi_1^{(3)}(m_{rd} + 1.5; 1, m_{rd}; m_{rd} + 2; \\ &\quad 2\lambda_{sd} \tilde{K}_{sd}, 2\lambda_{sd} (\tilde{K}_{sd} - m_{rd} \bar{\gamma}_{sd}/\bar{\gamma}_{rd}), \\ &\quad 2\lambda_{sd} \tilde{K}_{sd} C_{sdj}). \end{aligned} \quad (10)$$

B. Asymptotic ABER Analysis

In asymptotic analysis, we assume that the average SNR values for three links are sufficiently large i.e., $\bar{\gamma}_{kl} \gg 1$.

In case of TWDP fading, the MGF in (1) is approximated as

$$M_{\gamma_{kl}}^{\infty}(z) = \sum_{j=1}^{2L} 0.5\tilde{b}_{klj} \tilde{K}_{kl} \exp(-C_{klj}) (\bar{\gamma}_{kl} z)^{-1}, \quad (11)$$

and similarly for Nakagami- m fading, the MGF in (2) is approximated as

$$M_{\gamma_{kl}}^{\infty}(z) = (\bar{\gamma}_{kl} z / m_{kl})^{-m_{kl}}. \quad (12)$$

Under the high SNR assumption, we can use $1 - P_{sr}(e) \simeq 1$ and with the aid of (11) and (12), the asymptotic ABER represented as $P^{\infty}(e)$ can be given by

$$P^{\infty}(e) = P_{sr}^{\infty}(e)P_{sd}^{\infty}(e) + P_{mrc}^{\infty}(e), \quad (13)$$

where

$$P_w^{\infty}(e) = \frac{a}{\pi} \int_0^{\frac{\pi}{2}} M_{\gamma_w}^{\infty} \left(\frac{c^2}{2 \sin^2 \theta} \right) d\theta, \quad w \in \{sr, sd\} \quad (14)$$

$$P_{mrc}^{\infty}(e) = \frac{a}{\pi} \int_0^{\frac{\pi}{2}} M_{\gamma_{sd}}^{\infty} \left(\frac{c^2}{2 \sin^2 \theta} \right) M_{\gamma_{rd}}^{\infty} \left(\frac{c^2}{2 \sin^2 \theta} \right) d\theta. \quad (15)$$

The closed-form solutions of $P_w^{\infty}(e)$ and $P_{mrc}^{\infty}(e)$ are given in following subsections

1) *A Closed-Form Solution of $P_w^{\infty}(e)$:* Putting (11) into (14) and using substitution $u = \cos^2 \theta$ with the property of Beta function $B(x, y) = \int_0^1 u^{x-1} (1-u)^{y-1} du$, we derive the closed-form solution of $P_w^{\infty}(e)$ for TWDP faded link given as

$$P_w^{\infty}(e) = 0.25a\tilde{K}_w c^{-2}\bar{\gamma}_w^{-1} \sum_{j=1}^{2L} \tilde{b}_{wj} \exp(-C_{wj}). \quad (16)$$

2) *A Closed-Form Solution of $P_{mrc}^{\infty}(e)$:* Putting (11) and (12) into (15) and using substitution $u = \cos^2 \theta$ with the definition of Beta function, we derive the closed form solution of $P_{mrc}^{\infty}(e)$ for mixed fading scenario such as TWDP faded sd link and Nakagami- m faded rd link given as

$$P_{mrc}^{\infty}(e) = 0.5a\tilde{K}_{sd}\pi^{-1}c^{-2}\bar{\gamma}_{sd}^{-1} \left(2m_{rd}c^{-2}\bar{\gamma}_{rd}^{-1} \right)^{m_{rd}} \times B(0.5, m_{rd} + 1.5) \sum_{j=1}^{2L} \tilde{b}_{sdj} \exp(-C_{sdj}). \quad (17)$$

With the aid of (16) and (17), the asymptotic ABER expressions in (13) can be expressed by substituting $P_s = \sigma P$ and $P_r = (1-\sigma)P$ for $0 \leq \sigma \leq 1$, as

$$P^{\infty}(e) = \frac{\Omega_{rd}^{-m_{rd}} (P/N_0)^{-(1+m_{rd})}}{\beta_2^{-1} \sigma (1-\sigma)^{m_{rd}} \Omega_{sd}} + \frac{\beta_1 \Omega_{sr}^{-1}}{\sigma^2 \Omega_{sd}} \left(\frac{P}{N_0} \right)^{-2}, \quad (18)$$

where σ is power allocation factor, $\beta_1 = 0.0625a^2c^{-4} \times \tilde{K}_{sr}\tilde{K}_{sd} \sum_{j=1}^{2L} \tilde{b}_{srj} \exp(-C_{srj}) \sum_{j=1}^{2L} \tilde{b}_{sdj} \exp(-C_{sdj})$, and $\beta_2 = \frac{a\tilde{K}_{sd}}{2\pi c^2} \left(\frac{2m_{rd}}{c^2} \right)^{m_{rd}} B(0.5, m_{rd} + 1.5) \sum_{j=1}^{2L} \tilde{b}_{sdj} \times \exp(-C_{sdj})$.

C. Diversity Order and Coding Gain

The asymptotic ABER can be written as $P^{\infty}(e) = \left(G_c \left(\frac{P}{N_0} \right) \right)^{-G_d}$, where G_d and G_c are the diversity order and the coding gain, respectively. It can be noticed from (18) that the diversity order of the considered system is given by $G_d = 1 + \min\{1, m_{rd}\}$, whereas the coding gain G_c is equal to $\left(\frac{\beta_1 \Omega_{sr}^{-1}}{\sigma^2 \Omega_{sd}} + \frac{\beta_2 \Omega_{rd}^{-m_{rd}}}{\sigma (1-\sigma)^{m_{rd}} \Omega_{sd}} \left(\frac{P}{N_0} \right)^{-(m_{rd}-1)} \right)^{-\frac{1}{2}}$, $m_{rd} > 1$ or $\left(\frac{\beta_1 \Omega_{sr}^{-1}}{\sigma^2 \Omega_{sd}} \left(\frac{P}{N_0} \right)^{-(1-m_{rd})} + \frac{\sigma^{-1} \beta_2 \Omega_{rd}^{-m_{rd}}}{(1-\sigma)^{m_{rd}} \Omega_{sd}} \right)^{-\frac{1}{(1+m_{rd})}}$, $m_{rd} < 1$.

D. Optimal Power Allocation

It can be shown that the second derivative of $P^{\infty}(e)$ w.r.t σ is always greater than or equal to 0. Hence $P^{\infty}(e)$ is a convex function w.r.t. σ . The optimization problem is stated as [9] $\min_{\sigma} P^{\infty}(e)$, s.t. $0 < \sigma < 1$. Substituting $\sigma = \sigma_{opt}$ in the ‘first derivative of $P^{\infty}(e)$ w.r.t. σ ’ and equating the same to zero, we get the relation

$$\begin{aligned} -2\beta_1 \Omega_{rd}^{m_{rd}} (1 - \sigma_{opt})^{m_{rd}+1} (P/N_0)^{(m_{rd}-1)} \\ = \beta_2 \Omega_{sr} \sigma_{opt} (1 - (m_{rd} + 1)\sigma_{opt}). \end{aligned} \quad (19)$$

It can be observed from (19) that the σ_{opt} does not depend on Ω_{sd} , rather it depends on Ω_{sr} , Ω_{rd} , and P/N_0 . Moreover, the following are the range of allocated powers: $P/(1+m_{rd}) \leq P_s \leq P$, $0 \leq P_r \leq m_{rd}P/(1+m_{rd})$. It means that we should always allocate more power to ‘ s ’ and less power to ‘ r ’.

IV. NUMERICAL AND SIMULATION RESULTS

Numerical and Monte Carlo simulation results are presented and the impact of mixed TWDP and Nakagami- m fading parameters on the ABER performance is illustrated. In the evaluation and simulation, the power is equally allocated to the source device and the relay device and the mean power of each link is assumed to be unity, i.e., $\Omega_{sd} = \Omega_{sr} = \Omega_{rd} = 1$, unless stated otherwise. Numerical evaluation of the functions $\Phi_1^{(2)}(\cdot)$ and $\Phi_1^{(3)}(\cdot)$ are numerically computed by their finite integral representation.

Fig.1 shows the ABER for BPSK modulation ($a = 1$, $c = \sqrt{2}$) in five different practical fading scenarios: **Case 1** (Hyper Rayleigh - One-Sided Gaussian): $K_{sd} = K_{sr} = 10$, $\Delta_{sd} = \Delta_{sr} = 1$ (hyper-Rayleigh), $m_{rd} = 0.5$ (One-Sided Gaussian), **Case 2** (Rayleigh - Rayleigh): $K_{sd} = K_{sr} = 0$ (Rayleigh), $m_{rd} = 1$ (Rayleigh), **Case 3** (Rayleigh - Nakagami) $K_{sd} = K_{sr} = 0$ (Rayleigh), $m_{rd} = 2$ (Nakagami), **Case 4** (TWDP-Nakagami- m): $K_{sd} = K_{sr} = 4$, $\Delta_{sd} = \Delta_{sr} = 0.5$ (TWDP), $m_{rd} = 2.5$ (Nakagami- m), **Case 5** (Rician-Nakagami- m): $K_{sd} = K_{sr} = 4$, $\Delta_{sd} = \Delta_{sr} = 0$ (Rician), $m_{rd} = 2.5$ (Nakagami- m). It can be observed from Fig.1 that for all the cases there is a steady improvement of ABER with the increase of P/N_0 . **Case 1** performs worst and **Case 5** performs the best among five cases. It can be explained by the fact that the **Case 1** represents the worst fading scenario that can be modeled by mixed TWDP and Nakagami- m fading combinations. **Case 5** outperforms **Case 4** for fixed K and m . It is due to the closeness of the amplitudes of the two specular

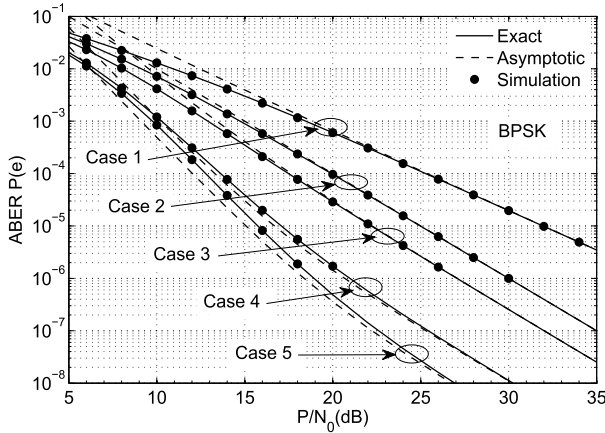


Fig. 1. ABER of BPSK for D2D communication using DF relaying in five different practical fading scenarios.

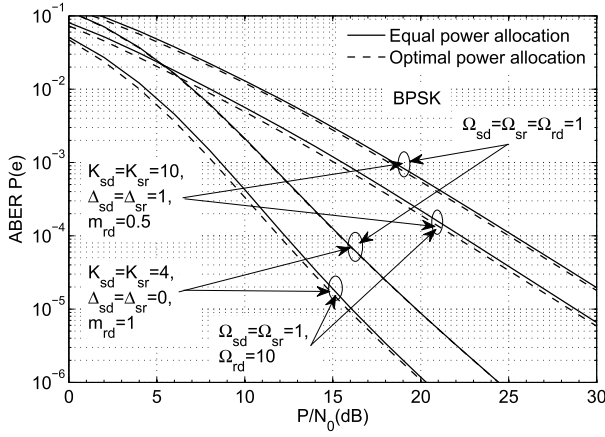


Fig. 2. ABER of BPSK for D2D communication using DF relaying with equal and optimal allocation.

TABLE I
 σ_{opt} IN (19) FOR BPSK, WITH $\Omega_{sd} = \Omega_{sr} = 1$, AND $P/N_0 = 40 \text{ dB}$

Ω_{rd}	$m_{rd} = 0.5$			$K_{sd} = K_{sr} = 4$ $\Delta_{sd} = \Delta_{sr} = 0$	
	$K_{sd} = K_{sr}$	$\Delta_{sd} = \Delta_{sr}$	σ_{opt}	m_{rd}	σ_{opt}
1	10	0.5	0.667	0.5	0.667
		1	0.669	1	0.514
	4	0.5	0.667	2	0.814
		1	0.668	2.5	0.907
10	10	0.5	0.667	0.5	0.667
		1	0.674	1	0.588
	4	0.5	0.668	2	0.954
		1	0.672	2.5	0.981

waves to each other, with increase in Δ . We notice from Fig. 1 that the exact analytical results match precisely with the Monte Carlo simulations and asymptotic ABER curves match closely with exact ABER curves at high SNR region. On examination, the ABER curves also confirm that the diversity order G_d is $1 + \min\{1, m_{rd}\}$ (i.e., $1.5 \leq G_d \leq 2$).

Table I tabulates the σ_{opt} to the source device s for BPSK as a function of Ω_{rd} , $K_{sd} = K_{sr}$, $\Delta_{sd} = \Delta_{sr}$, and m_{rd} at $P/N_0 = 40 \text{ dB}$. The values of σ_{opt} for any value of channel parameters of mixed TWDP and Nakagami- m fading channels can be obtained by solving (19) using MATHEMATICA

software. It can be observed from Fig. 2 and Table I that when fading parameters and mean powers of links are highly unbalance, an optimal power allocation is of advantageous. This is useful from application point of view in a limited power scenario, as in sensor network transceivers, where it is required to maintain a desired ABER. Nodes can convey information through feedback paths to modify the transmitted power suitably and hence optimize on battery consumption. This technique, if used adaptively would improve the average life of sensors.

V. CONCLUSION

The performance of D2D communication using selective DF relaying in mixed TWDP and Nakagami- m fading channels is analyzed. New closed-form expressions for exact and asymptotic ABERs are derived. Besides, the diversity order, the coding gain, and the optimal power allocation factor is obtained. The diversity order of the system has been obtained to be in the range 1.5 to 2. The derived analytical results include various practical fading scenarios as special cases.

REFERENCES

- [1] M. Alam, D. Yang, J. Rodriguez, and R. A. Abd-Alhameed, "Secure device-to-device communication in LTE-A," *IEEE Commun. Mag.*, vol. 52, no. 4, pp. 66–73, Apr. 2014.
- [2] H. Nishiyama, M. Ito, and N. Kato, "Relay-by-smartphone: Realizing multi-hop device-to-device communications," *IEEE Commun. Mag.*, vol. 52, no. 4, pp. 56–65, Apr. 2014.
- [3] A. Nosratinia, T. E. Hunter, and A. Hedayat, "Cooperative communication in wireless networks," *IEEE Commun. Mag.*, vol. 42, no. 10, pp. 74–80, Oct. 2004.
- [4] G. D. Durgin, T. S. Rappaport, and D. A. de Wolf, "New analytical models and probability density functions for fading in wireless communications," *IEEE Trans. Commun.*, vol. 50, no. 6, pp. 1005–1015, Jun. 2002.
- [5] M. K. Simon and M.-S. Alouini, *Digital Communication Over Fading Channels*, 2nd ed. New York, NY, USA: Wiley, 2005.
- [6] P. Kyösti et al., "WINNER II channel models (V1.1)," WINNER II, Munich, Germany, Tech. Rep. IST-4-027756 WINNER II D1.1.1, Sep. 2007. [Online]. Available: <http://www.ist-winner.org/WINNER2-Deliverables/D1.1.1.pdf>
- [7] N. Kapucu, M. Bilim, and I. Develi, "Outage probability analysis of dual-hop decode-and-forward relaying over mixed Rayleigh and generalized gamma fading channels," *Wireless Pers. Commun.*, vol. 71, no. 2, pp. 947–954, 2012.
- [8] C. Yang, W. Wang, W. Zhao, and M. Peng, "Opportunistic decode-and-forward cooperation in mixed Rayleigh and Rician fading channels," *ETRI J.*, vol. 33, no. 2, pp. 287–290, 2011.
- [9] Y. Lee and M.-H. Tsai, "Performance of decode-and-forward cooperative communications over Nakagami- m fading channels," *IEEE Trans. Veh. Technol.*, vol. 58, no. 3, pp. 1218–1228, Mar. 2009.
- [10] Y. Lu and N. Yang, "Symbol error rate of decode-and-forward relaying in two-wave with diffuse power fading channels," *IEEE Trans. Wireless Commun.*, vol. 11, no. 10, pp. 3412–3417, Oct. 2012.
- [11] D. Dixit and P. R. Sahu, "Exact closed-form ABER for multi-hop regenerative relay systems over κ - μ fading," *IEEE Wireless Commun. Lett.*, vol. 6, no. 2, pp. 246–249, Apr. 2017.
- [12] P. Kumar and K. Dhaka, "Performance analysis of a decode-and-forward relay system in κ - μ and η - μ fading channels," *IEEE Trans. Veh. Technol.*, vol. 65, no. 4, pp. 2768–2775, Apr. 2016.
- [13] M. K. Fikadu, P. C. Sofotasios, S. Muhamad, Q. Cui, G. K. Karagiannidis, and M. Valkama, "Error rate and power allocation analysis of regenerative networks over generalized fading channels," *IEEE Trans. Commun.*, vol. 64, no. 4, pp. 1751–1768, Apr. 2016.
- [14] D. Dixit and P. R. Sahu, "Performance of dual-hop DF relaying systems with QAM schemes over mixed η - μ and κ - μ fading channels," *Trans. Emerg. Telecommun. Technol.*, vol. 28, no. 11, pp. 1–13, Apr. 2017.
- [15] H. Exton, *Multiple Hypergeometric Functions and Applications*. New York, NY, USA: Wiley, 1976.